

# Parallel Imaging Using a 3D Concentric Cylinders Trajectory

K. Kwon<sup>1</sup>, H. H. Wu<sup>1,2</sup>, M. Lustig<sup>1,3</sup>, and D. G. Nishimura<sup>1</sup>

<sup>1</sup>Electrical Engineering, Stanford University, Stanford, CA, United States, <sup>2</sup>Cardiovascular Medicine, Stanford University, Stanford, CA, United States, <sup>3</sup>Electrical Engineering and Computer Science, University of California at Berkeley, Berkeley, CA, United States

**Introduction:** 3D stack-of-rings and 3D concentric cylinders are two different extensions of the 2D concentric rings trajectory for 3D imaging. The 3D stack-of-rings trajectory directly inherits the centric-ordered sampling scheme and shorter scan times from the 2D concentric rings [1,2]. The 3D concentric cylinders trajectory is similar to stack-of-rings, but it also has a unique property that leads to fewer excitations than a comparable 3DFT trajectory and benign off-resonance effects [3-5]. Recently, an efficient parallel imaging strategy for the 3D stack-of-rings trajectory was developed, which further enhances its flexible trade-offs between image quality and scan time [6]. In this work, we applied a similar parallel imaging strategy to 3D concentric cylinders, which decomposes the 3D non-Cartesian parallel imaging reconstruction into a series of 2D Cartesian reconstructions. Combined with the centric-ordered sampling scheme, this trajectory can be used to efficiently capture transient responses in a magnetization-prepared sequence.

**Methods:** A 3D concentric cylinders trajectory derives from a 2D concentric rings trajectory by adding a constant  $G_z$  gradient during the readout interval [3-5]. Once the radius (in  $k_x, k_y$ ) and the height (in  $k_z$ ) of the outermost cylinder are chosen based on the desired spatial resolution, the number of uniformly-spaced concentric cylinders ( $N_c$ ) determines the in-plane FOV, while the number of interleaves per cylinder ( $N_{intlv}$ ) and the number of revolutions per interleaf ( $N_{rev}$ ) determine the slab-direction FOV and the number of slices ( $N_{slice} = N_{intlv} \times N_{rev}$ ) (Fig. 1a). If the design meets two conditions: 1)  $N_{intlv} = \text{even number}$ , 2) the number of sampling points per interleaf  $N_{samp} = m \times N_{slice}$  ( $m$ : positive integer), then the  $k$ -space data can be reformatted as a set of 2D Cartesian spoke-planes, which cut through the cylinders acquisition along full-diameter spokes (Fig. 1b). Although the samples in different spoke-planes are slightly shifted with respect to each other in the  $k_z$  direction due to the constant  $G_z$  gradient, data points in each spoke-plane remain on a 2D Cartesian grid (Fig. 1c), and the amount of maximum shift is at most  $1/N_{slice}$  of the maximum  $k_z$  extent. Thus, it is possible to apply a 2D Cartesian parallel imaging strategy for each spoke-plane. Undersampling is achieved by acquiring interleaves fewer than the  $N_{intlv}$  necessary for full-FOV in the slab direction. Interleaves of inner cylinders are still fully acquired for auto-calibration (Fig. 1d). After missing points in each spoke-plane are filled using 2D Cartesian reconstruction, 3D gridding reconstruction is performed for each coil. Data from multiple coils are combined using a sum-of-squares method.

**Results and Discussions:** To demonstrate the feasibility of the proposed parallel imaging strategy with 3D concentric cylinders, a lower extremity scan was performed on a GE Excite 1.5 T whole-body scanner with an 8-channel knee coil. Gradients were designed to provide resolution =  $1 \times 1 \times 2 \text{ mm}^3$  and FOV =  $20 \times 20 \times 13 \text{ cm}^3$  (matrix size =  $192 \times 192 \times 64$ ) using  $N_c = 96$ ,  $N_{slice} = 64$ ,  $N_{intlv}/N_{rev} = 16/4$ . Readout bandwidth =  $\pm 125 \text{ kHz}$  was used, which yielded  $N_{samp} = 1792$  points ( $28 \times N_{slice}$ ) per interleaf. This 3D interleaved concentric cylinders trajectory was incorporated into an SSFP sequence with TE/TR =  $2/14 \text{ ms}$  and flip angle =  $60^\circ$ . The scan time for each fully acquired dataset was 30 s. This dataset was reformatted as 224 spoke-planes with matrix size  $191 \times 64$  each. Then, it was retrospectively undersampled with a reduction factor  $R = 2$ , which corresponds to acquiring even-numbered interleaves for odd-numbered cylinders and vice versa (Fig. 1d). GRAPPA-based reconstruction [7,8] was performed for each spoke-plane with a fully sampled auto-calibration region (Fig. 1d) of 8 cylinders ( $15 \times 64$  in each spoke-plane) and a  $5 \times 5$  interpolation kernel. 64 slices were reconstructed by 3D gridding for each coil. Figure 2 shows representative images from fully sampled reconstruction, a zero-filled reconstruction of the undersampled dataset, and finally the parallel imaging reconstruction for the undersampled dataset. The parallel imaging result closely matches the fully sampled result (Fig. 2c), while the zero-filled reconstruction exhibits aliasing (white arrows, Fig. 2b). This demonstrates that the proposed parallel imaging reconstruction is feasible for the 3D interleaved concentric cylinders, and the original scan time (30 s) can be reduced to about 15 s if the  $R = 2$  undersampling pattern is used.

**Conclusion:** The 3D interleaved concentric cylinders trajectory has a sampling geometry that can be designed to be combined with an efficient parallel imaging strategy, reformatting the 3D non-Cartesian data as a set of 2D Cartesian spoke-planes. With a factor of  $2N_{rev}$  fewer excitations than a comparable 3DFT acquisition even before parallel imaging is applied [5], this centric-ordered 3D trajectory is highly efficient for magnetization-prepared imaging, such as for non-contrast-enhanced MR angiography based on SSFP [5]. If combined with other fast imaging methods such as fully 3D parallel imaging and compressed sensing or enhanced with variable density sampling, this trajectory can yield even shorter scan times.

**References:** [1] Wu, MRM 59:102, 2008. [2] Wu, MRM 63:1210, 2010. [3] Mugler, SMR, p.483, 1995. [4] Ruppert, ISMRM, p.208, 2003.

[5] Kwon, ISMRM, p.4973, 2010. [6] Wu, ISMRM, p.2878, 2010. [7] Griswold, MRM 47:1202, 2002. [8] <http://www.eecs.berkeley.edu/~mlustig>

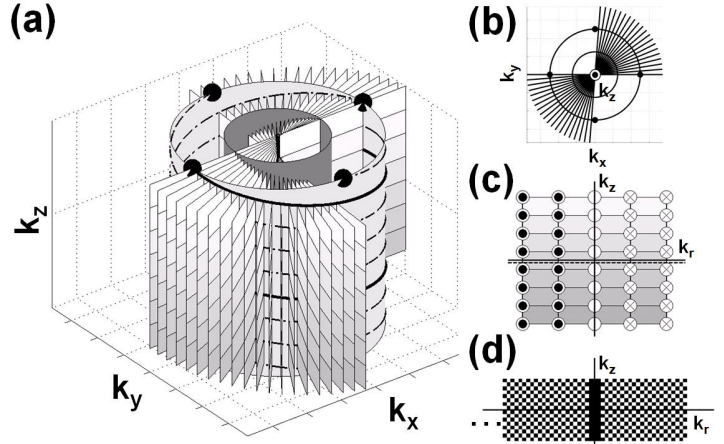


**Fig. 1.** (a)  $k$ -space trajectory of 3D concentric cylinders with  $N_c = 3$  (radius of the innermost cylinder is 0),  $N_{intlv} = 4$  (black spheres at the top are starting points of helical interleaves covering the outermost cylinder),  $N_{rev} = 2$ ,  $N_{slice} = 8$ , and  $N_{samp} = 160$ . Depicted are 20 ( $= m$ ) of a total of 40 full-diameter spoke-planes, which are slightly shifted in the  $k_z$  direction. (b) View from  $k_z$  axis. (c) View of a spoke-plane with data points on a 2D Cartesian grid ( $k_r$ : the radial axis of each spoke-plane, which is slightly shifted from  $k_z = 0$ . left side: interleaves coming out, right: going in). (d) Uniform undersampling pattern ( $R = 2$ ) with fully sampled center (black: sampled) for auto-calibration.

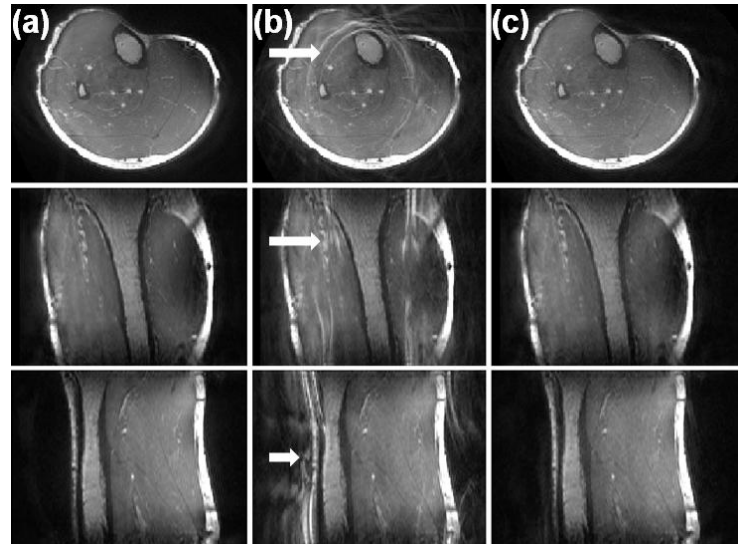


**Fig 2.** Representative axial, coronal, and sagittal images of the calf. (a) fully sampled reconstruction, (b) undersampling with zero-filled reconstruction, (c) undersampling with parallel imaging reconstruction.